Multiscale simulation of the heat and mass transfer with Brinkman model

Multiscale simulation of the heat and mass transfer with Brinkman model

Valentin Alekseev[1], Maria Vasilyeva[2], Vasily Vasiliev[3]

[1]Multiscale model reduction Laboratory, North-Eastern Federal University, Yakutsk, Russia
[2]North-Eastern Federal University, Yakutsk, Russia, Institute for Scientific Computation, Texas A&M University, College Station, TX, USA
[3]North-Eastern Federal University, Yakutsk, Russia

E-mail: alekseev.valen@mail.ru

Abstract. In this work, we consider a heat and mass transfer problem in heterogeneous media. Mathematical model is described by a system of equations for temperature, pressure and velocity. For simulations of the flow problem in domain with low permeable obstacles, we use a Brinkman model. Fine grid approximation is constructed based on the discontinuous Galerkin (IPDG) method for heat transfer and flow problems. For coarse grid approximation of the flow problem, we use a Generalized Multiscale Discontinuous Galerkin Method. Numerical results are presented for a two-dimensional model problem with different number of the multiscale basis functions.

1. Problem formulation

In this work, we consider the transport and flow problems in domain with a low permeable obstacles $\Omega = \Omega_1 \cup \Omega_2$, where Ω_1 is the free flow domain and Ω_2 is the obstacles subdomain. Transport problem simulate a heat transfer in the heterogeneous domains with free flow in the subdomain Ω_1. For the simulation of the flow in the heterogeneous domains with the free flow in subdomain Ω_1 and Darcy's flow in low permeable obstacles, we use a Brinkman model (Darcy-Stokes-Brinkman model) [1, 2, 3, 4]. Such mathematical models are used, for example, to describe a complex processes in the porous media at the pore-level [5, 6, 7, 8, 9].

We consider flow and heat transfer problem in heterogeneous domain $\Omega = \Omega_1 + \Omega_2$. The flow problem is described by the Brinkman model

$$\begin{aligned} \mu \Delta u - \nabla p + A u = 0, \quad x \in \Omega, \\ \nabla \cdot u = 0, \quad x \in \Omega, \end{aligned} \tag{1}$$

with following boundary conditions

$$u = g, \quad x \in \Gamma_L, \quad (\mu \nabla u - p\mathcal{I}) \cdot n = 0, \quad x \in \Gamma_R, \quad u = 0, \quad x \in \Gamma_T \cup \Gamma_B,$$

where μ is the viscosity, p is the pressure, $A = k^{-1}$. Here permeability k in the obstacles domain Ω_2 is defined using Carman-Kozeny equation

$$A = \begin{cases} 0, & x \in \Omega_1, \\ -C\dfrac{(1-\epsilon)^2}{\epsilon^3 + b}, & x \in \Omega_2, \end{cases}$$

where C is the constant accounting for the mushy-region morphology, ϵ is the porosity, b is a constant introduced to avoid division by zero.

The heat transfer equation is described by a convection-diffusion equation with given velocity field u

$$\alpha\left(\frac{\partial T}{\partial t} + u \cdot \operatorname{grad} T\right) - \operatorname{div}\cdot(\lambda \operatorname{grad} T) = 0, \quad x \in \Omega \tag{2}$$

with initial condition $T = T_0$ and boundary conditions

$$T = T_1, \quad x \in \Gamma_L, \quad -\lambda\frac{\partial T}{\partial n} = 0, \quad x \in \Gamma_R \cup \Gamma_T \cup \Gamma_B,$$

where $\partial\Omega = \Gamma_L \cup \Gamma_R \cup \Gamma_T \cup \Gamma_B$.

For the coefficients of the equation, we have the following relationships

$$\alpha = \begin{cases} \rho_w c_w, & x \in \Omega_1, \\ \rho_{sc} c_{sc}, & x \in \Omega_2, \end{cases} \quad \lambda = \begin{cases} \lambda_w, & x \in \Omega_1, \\ \lambda_{sc}, & x \in \Omega_2, \end{cases}$$

where ρ_w, c_w, λ_w and ρ_{sc}, c_{sc}, λ_{sc} are density, specific heat capacity and thermal conductivity of water and grains, respectively.

2. Fine grid approximation

To approximate the problem with respect to spatial variables, we use the discontinuous Galerkin method (IPDG) for both heat transfer and flow equations (2) and (1). For a classic approximation, we construct a sufficiently fine grid that resolve all small scale heterogeneities on the grid level. Let $\mathcal{T}^h$ be a triangulation of the computational domain Ω and Γ^h be the set of all faces between the elements $\mathcal{T}^h$. On the edge $E \in \Gamma^h$ between the elements K_1 and K_2, we define an average and the jump of the function u

$$\{u\} = \frac{u|_{K_1} + u|_{K_2}}{2}, \quad [u] = u|_{K_1} - u|_{K_2}.$$

The fine scale velocity space $V^h = \{v \in L^2(\Omega) : v|_K \in (\mathbb{P}_1(K))^2, \forall K \in \mathcal{T}^h\}$ contains functions which are piecewise linear in each fine-grid element K and discontinuous across coarse grid edges. For the pressure, we use the space of piecewise constant functions Q^h. We have following variational formulation for the flow problem (1): find $(u, p) \in V^h \times Q^h$ such that

$$\begin{aligned} a_{DG}(u, v) + b_{DG}(p, v) = 0, \quad \forall v \in V^h \\ b_{DG}(u, q) = 0, \quad \forall r \in Q^h, \end{aligned} \tag{3}$$

where

$$a_{DG}(u, v) = \sum_{K\in\mathcal{T}^h} \int_K (\mu\, \nabla u \cdot \nabla v + A\, u\, v) dx - \sum_{E\in\Gamma_h} \int_E \Big([\mu\, u \cdot n]\, \{v\} - \{\mu\, v \cdot n\}\, [u] - \{\mu\} \frac{\gamma_u}{h}\, [u]\, [v] \Big)\, ds,$$

$$b_{DG}(u, p) = \sum_{K\in\mathcal{T}^h} \int_K p \nabla u dx + \sum_{E\in\Gamma_h} \int_E \{p\} [u \cdot n]\, ds,$$

where γ_u is the penalty parameter and n is the unit normal to the edge E.

The variational formulation of the transport equation (2) using the discontinuous Galerkin method (IPDG, Interior Penalty Discontinuous Galerkin) is defined as follows: find $T^{n+1} \in W^h$ such that

$$\sum_{K\in\mathcal{T}^h}\int_K\left(\alpha\frac{T^{n+1}-T^n}{\tau}\,r+\alpha\,u\cdot\nabla T^{n+1}\,r+\lambda\,\nabla T^{n+1}\cdot\nabla r\right)dx+\sum_{E\in\Gamma_h}\int_E[T^{n+1}u\cdot n][r]\,ds$$
$$-\sum_{E\in\Gamma_h}\int_E\left(\{\lambda\,\nabla r\}\cdot[T^{n+1}\,n]-\{\lambda\,\nabla T^{n+1}\}\cdot[r\,n]+\{\lambda\}\frac{\gamma_T}{h}\cdot[T^{n+1}\,n]\,[r\,n]\right)ds=0,\quad\forall r\in W^h, \tag{4}$$

where γ_T is the penalty parameter and $W^h=\{v\in L^2(\Omega):\,v|_K\in(\mathbb{P}_1(K))^2,\,\forall K\in\mathcal{T}^h\}$. Here, we use an implicit scheme for approximation by time with time step τ.

Next, we describe construction of the coarse grid approximation using Generalized finite element method for flow problem. Note that, we solve a transport problem on the fine grid.

3. Multiscale method

In this section, we describe construction of the coarse grid approximation using Generalized finite element method for flow problem. Note that, we solve a transport problem on the fine grid. Let $\mathcal{T}^H$ be a coarse grid of domain Ω with mesh size H and $\mathcal{E}^H$ be the set of all facets of the coarse grid in $\mathcal{T}^H$. For the pressure approximation, we use the piecewise constant function space Q^H over the coarse cells. We define V^H as the multiscale velocity space, which contains a set of basis functions supported in each coarse block K. [10, 11, 12, 13].

We construct a multiscale space for the velocity

$$V^H=\operatorname{span}\{\psi_i\}_{i=1}^{N_u},\quad Q^H=\{r\in L^2(\Omega):\,r|_K\in P^0(K),\,\forall K\in\mathcal{T}_H\}$$

and for the pressure, we use the space of piecewise constant functions over the coarse triangulation, $N_u=\dim(V^H)$ is the number of basis functions and $N_p=\dim(Q^H)$ is equal to the number of coarse grid cells.

For the coarse grid approximation, we use a Discontinuous Galerkin(DG) approach and have following variational formulation: find $(u_H,p_H)\in V^H\times Q^H$ such that

$$\begin{aligned}a_{\mathrm{DG}}(u_H,v)+b_{\mathrm{DG}}(p_H,v)&=f(v)\quad\forall v\in V^H,\\ b(u_H,q)&=0,\quad\forall q\in Q^H.\end{aligned} \tag{5}$$

For construction of the multiscale space for the velocity, we solve a spectral problem to select dominant modes of the snapshot space. We construct local snapshot basis in each coarse block $K_i,(i=1,\cdots,N)$, where N is the number of coarse blocks in Ω. The local snapshot space consists of functions which are solutions $\phi_l^i\in V^h(K_i)$ of

$$\begin{aligned}a_{\mathrm{DG}}(\phi_l^i,v)+b_{\mathrm{DG}}(\eta,v)&=0\quad\forall v\in V^h(K_i),\\ b(\phi_l^i,q)&=\int_{K_i}c\,q\,dx,\quad\forall q\in Q^h(K_i).\end{aligned} \tag{6}$$

with $\phi_l^i=\delta_i^l$ on ∂K_i $(l=1,\cdots,J_i)$, where J_i is the number of fine grid nodes on the boundary of K_i, and δ_i^l is the discrete delta function defined on ∂K_i. Here, c is chosen by the compatibility

condition, $c = \frac{1}{|K_i|}\int_{\partial K_i} \delta_i^l \cdot n\, ds$. Next, we form a local snapshot space in K_i using the all local solutions $V^{i,\text{snap}} = \{\phi_l^i : 1 \le l \le J_i\}$ and define projection matrix to the snapshot space $R_{i,\text{snap}} = \left[\phi_1^i, \ldots, \phi_{J_i}^i\right]$.

To reduce size of the snapshot space, we solve following local spectral problem

$$A^{i,\text{snap}}\psi_k^{i,\text{snap}} = \lambda_k S^{i,\text{snap}}\psi_k^{i,\text{snap}}, \tag{7}$$

where $A^{i,\text{snap}} = R_{i,\text{snap}}A^i R_{i,\text{snap}}^T$, $S^{i,\text{snap}} = R_{i,\text{snap}}S^i R_{i,\text{snap}}^T$. Here A^i is the matrix representation of the bilinear form $a_i(u,v)$ and S^i is the matrix representation of the bilinear form $s_i(u,v)$

$$a_i(u,v) = \int_{K_i} \mu\, \nabla u \cdot \nabla v\, dx, \quad s_i(u,v) = \int_{\partial K_i} u \cdot v\, dx.$$

We arrange the eigenvalues in increasing order and choose the first eigenvectors corresponding to the first M_i the smallest eigenvalues $\psi_k^i = R_{i,\text{snap}}\psi_k^{i,\text{snap}}$ as the basis functions ($k = 1, ..., M_i$)

$$V^H = \text{span}\{\psi_k^i : 1 \le i \le N_e,\, 1 \le k \le M_i\},$$

This multiscale space will be used as the approximation space for the velocity.

4. Numerical results

We consider numerical simulation using the proposed models in heterogeneous computational domain $\Omega = [0,1]^2$ (see Figure 1). The fine grid contains 89778 vertices, 30127 facets and 59562 triangular cells. We consider two coarse grids: (1) 5×5 grid with 36 vertices, 60 facets and 25 cells; (2) 10×10 grid with 121 vertices, 220 facets and 100 cells. We set $\mu = 1.0$, $C = 1.0$, $\epsilon = 10^{-5}$, $b = 10^{-6}$, $\rho_w = 1000$, $c_w = 4200$, $\lambda_w = 560$, $\rho_{sc} = 1260$, $c_{sc} = 840$, $\lambda_{sc} = 1100$, $g = (1.0, 0.0)$, $T_0 = 1$ and $T_1 = 10$. We simulate for $t = 0.5$ with 50 time steps.

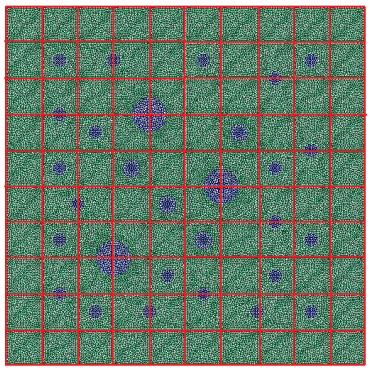

Figure 1. Computational domain with coarse and fine grids

To compare the results, we use the relative L_2 and H_1 errors between fine-scale solutions v_f and multiscale solutions v_{ms} for velocity ($e_{L_2}^u$ and $e_{H_1}^u$). For pressure, we use a L_2 errors on the fine and coarse grids ($e_{L_2}^p$ and $e_{L_2}^{\bar{p}}$). For temperature, we calculate L_2 error on the fine grid using fine scale and multiscale velocity ($e_{L_2}^T$).

The results of calculations are shown in Figure 2, where we present the X and Y components of velocity, pressure and temperature distributions for fine grid and multiscale solutions.

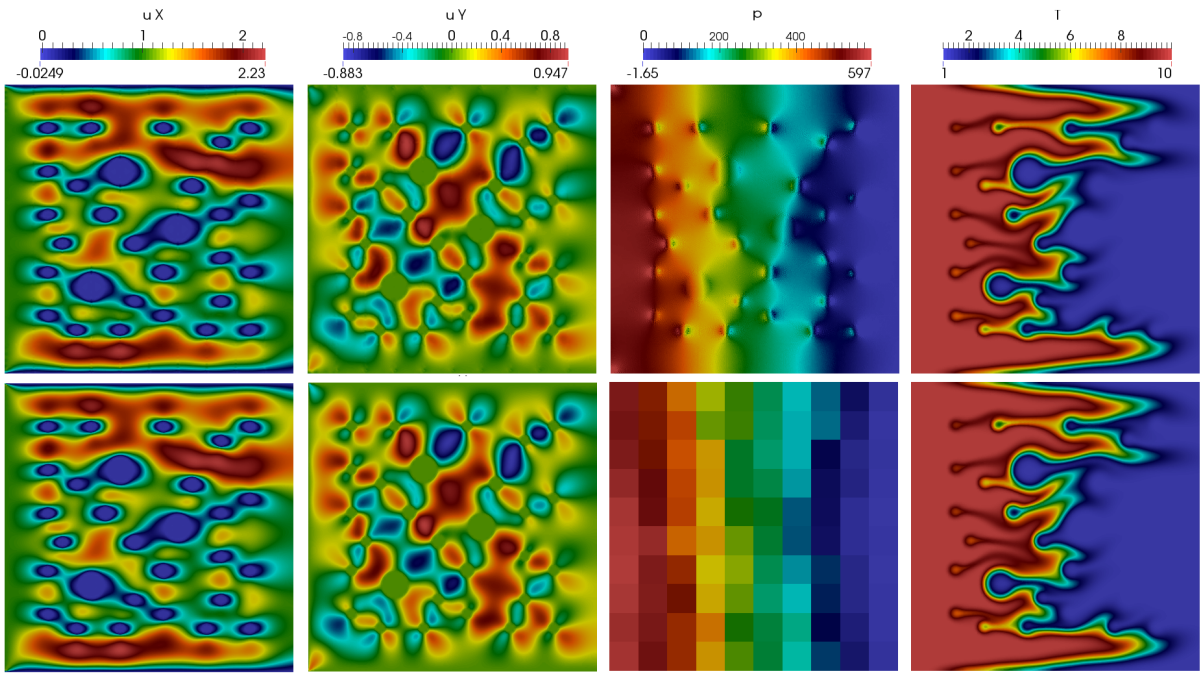

Figure 2. The distribution of the velocity (u_x and u_y), pressure and temperature (from left to right). Top: Fine grid solution. Bottom: Multiscale solution.

5×5						
M	DOF_c	$e^u_{L_2}$ (%)	$e^u_{H_1}$ (%)	$e^p_{L_2}$ (%)	$e^{\overline{p}}_{L_2}$ (%)	$e^T_{L_2}$ (%)
10	275	43.059	78.449	732.669	41.409	28.847
20	525	15.426	39.407	38.187	0.19	8.598
30	775	8.424	29.258	20.21	0.026	5.610
40	1025	5.317	24.173	16.595	9.1e-03	3.251
60	1525	3.044	18.645	14.723	1.79e-03	1.976
10×10						
10	1100	22.24	51.489	91.398	4.079	12.705
20	2100	6.081	30.154	20.233	0.054	3.792
30	3100	3.683	23.081	15.025	0.013	2.712
40	4100	2.673	19.833	13.572	9.04e-03	1.888
60	6100	2.154	17.056	12.604	4.87e-03	1.497

Table 1. Relative errors for velocity and pressure with different number of multiscale basis functions for 5x5 and 10x10 meshes

Calculation was performed using 60 multiscale basis functions for the velocity filed. Temperature distribution is presented at final time for solution on the fine grid with fine scale and multiscale velocity field. Relative errors are presented in Table 1 for 5×5 and 10×10 coarse grids. We observe that the velocity L_2 error reduce from 43% to 3% and the pressure coarse grid error reduce from 41% to 0.00179% for 5×5 grids, when we use 10 and 60 multiscale velocity basis functions respectively. On the 10×10 coarse grid, the velocity L_2 error reduce from 22% to 2% and the pressure coarse grid error reduce from 4% to 0.00487%, when we use 10 and 60 multiscale

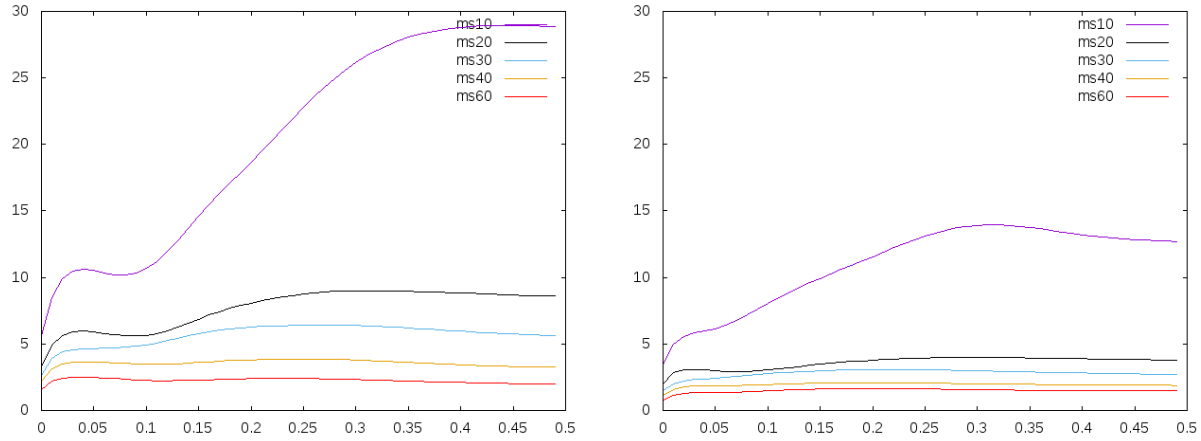

Figure 3. The L_2 error between the fine-scale and multiscale solution of the temperature. (Left: Error for 5x5 meshes. Right: Error for 10x10 meshes.)

velocity basis functions respectively. In Figure 3, we present dynamic of the relative L_2 error for temperature, where we obtain a good solutions using sufficient number of the multiscale basis functions for accurate approximation of the velocity field.

5. Acknowledgments

The work are supported by the mega-grant of the Russian Federation Government N14.Y26.31.0013 and RSF N19-11-00230.

References

[1] Young T. J., Vafai K. Convective flow and heat transfer in a channel containing multiple heated obstacles *International Journal of Heat and Mass Transfer (Vol. 41, No. 21, pp. 3279-3298)* 1998.
[2] Hsu C. T., Cheng P. The Brinkman model for natural convection about a semi-infinite vertical flat plate in a porous medium *International Journal of Heat and Mass Transfer (Vol. 28, No. 3, pp. 683-697)* 1985.
[3] Lesinigo M., DAngelo C., Quarteroni A. A multiscale DarcyBrinkman model for fluid flow in fractured porous media *Numerische Mathematik (Vol. 117, No. 4, pp. 717-752)* 2011.
[4] Khaled A. R. A., Vafai K. The role of porous media in modeling flow and heat transfer in biological tissues *International Journal of Heat and Mass Transfer (Vol. 46, No. 26, pp. 4989-5003)* 2003.
[5] Chung E. T., Vasilyeva M., Wang Y. A conservative local multiscale model reduction technique for Stokes flows in heterogeneous perforated domains *Journal of Computational and Applied Mathematics (Vol. 321, pp. 389-405)* 2017.
[6] Chung, E. T., Efendiev, Y., Li, G., Vasilyeva, M. Generalized multiscale finite element methods for problems in perforated heterogeneous domains. *Applicable Analysis (Vol. 95, No. 10, pp. 2254-2279)* 2016.
[7] Spiridonov, D., Vasilyeva, M., Leung, W. T. A Generalized Multiscale Finite Element Method (GMsFEM) for perforated domain flows with Robin boundary conditions. *Journal of Computational and Applied Mathematics (Vol. 357, pp. 319-328)* 2019.
[8] Vasilyeva, M., Chung, E. T., Leung, W. T., Wang, Y., Spiridonov, D. Upscaling method for problems in perforated domains with non-homogeneous boundary conditions on perforations using Non-Local Multi-Continuum method (NLMC). *Journal of Computational and Applied Mathematics (Vol. 357, pp. 215-227)* 2019.
[9] Alekseev, V., Gavrileva, U., Spiridonov, D., Tyrylgin, A., Vasilyeva, M Numerical simulation of the transport and flow problems in perforated domains using generalized multiscale finite element method *AIP Conference Proceeding AIP Publishing (Vol. 2025, No. 1, pp. 100001)* 2018.

[10] Chung, E. T., Efendiev, Y., Vasilyeva, M., Wang, Y. A multiscale discontinuous Galerkin method in perforated domains. *In Proceedings of the Institute of Mathematics and Mechanics (Vol. 42, No. 2, pp. 212-229)* 2016.

[11] Chung, E. T., Vasilyeva, M., Wang, Y. A conservative local multiscale model reduction technique for Stokes flows in heterogeneous perforated domains. *Journal of Computational and Applied Mathematics (Vol. 321, pp. 389-405)* 2017.

[12] Stepanov S., Vasilyeva M., Vasilev V. I. Generalized multiscale discontinuous Galerkin method for solving the heat problem with phase change *Journal of Computational and Applied Mathematics (Vol. 340, pp. 645-652)* 2018.

[13] Tyrylgin A., Vasilyeva M., Brown D. Generalized Multiscale Finite Element Method for Poroelasticity Problems in Heterogeneous Media *International Conference on Finite Difference Methods Springer, Cham (pp. 566-573)* 2018.

[14] Gavrileva U. et al. Generalized Multiscale Discontinuous Galerkin Method for Helmholtz Problem in Fractured Media *International Conference on Finite Difference Methods Springer, Cham (pp. 250-257)* 2018.